Electronic Supplementary Material (ESI) for Dalton Transactions.

Supporting Information:

The Modular Synthesis of Rare Earth-Transition Metal Heterobimetallic Complexes Utilizing a Redox-Active Ligand

James R. Hickson,[a,b] Samuel J. Horsewill,[a] Christopher Bamforth,[a] Jake McGuire,[a] Stephen Sproules,[a] Claire Wilson[a] and Joy H. Farnaby[a]*

[a] School of Chemistry, WestCHEM, University of Glasgow, Glasgow, UK.

[b] Department of Chemistry, Imperial College London, South Kensington, London, UK.

Contents

Additional Synthetic Details:

S1. Synthesis of 1,10-Phenanthroline-5,6-Dione (pd)

A modified version of the synthesis reported by Yamada and co-workers was followed.[1]

To frozen 97% H_2SO_4 (100 mL, 1.88 mol), 1,10-phenanthroline (10 g, 47.6 mmol) and KBr (20 g, 168 mmol) were added. The mixture was allowed to warm to room temperature over 30 m, giving an orange paste. A reflux condenser was fitted, and 65% HNO_3 (50 mL, 1.20 mol) was added dropwise over 30 m. The mixture was heated at 130 ^oC for 16 h, after which evolution of bromine was complete. The mixture was poured over ice, and $NaHCO_3$ (37 g) was added in small portions with stirring until pH 7 was reached. The product was filtered, extracted with CH_2Cl_2 (5 x 20 mL), dried over $MgSO_4$ and the solvent removed *in vacuo*. The yellow product was washed with MeOH (3 x 10 mL) and dried *in vacuo*, yielding 1,10-phenanthroline-5,6-dione (8.1 g, 38.5 mmol, 81% yield). ^1H NMR ($CDCl_3$): δ 7.69 (2H, dd, *J* = 7.9, 4.7 Hz, $C^{3,8}$-**H**) 8.50 (2H, dd, *J* = 7.9, 1.8 Hz, $C^{4,7}$-**H**) 9.12 (2H, dd, *J* = 4.7, 1.8 Hz, $C^{2,9}$-**H**) ppm. ^{13}C NMR ($CDCl_3$): δ 178.7, 156.41, 137.31, 128.06, 125.62 ppm. IR (ATR): 3351(w), 3075(w), 3021(w), 1678(s, υCO), 1558 (s), 1416 (m), 1272 (s), 1201 (m) cm^{-1}. λ_{max} (MeCN)/nm (ε/M^{-1} cm^{-1}): 243 (4 510), 256 (3 748).

S2. Synthesis of $Y(OTf)_3$

A modified version of the synthesis reported by Fukuzumi and co-workers was followed.[2]

Y_2O_3 (4.51 g, 20 mmol) was added to a solution of 50% v:v triflic acid in water (21 mL, 120.1 mmol). The resulting suspension was heated at reflux for 16 h, until Y_2O_3 was completely consumed. The solution was reduced in volume by half and the resulting crystals collected by suction filtration. $[Y(OTf)_3(H_2O)_x]$ was washed with hexane until white (4 x 5 mL, off-white colouration is an indicator of remaining triflic acid). $Y(OTf)_3(H_2O)_x$ was ground with a pestle and mortar, and dehydrated *in vacuo* for 48 h at 220 ^oC to give $Y(OTf)_3$ as a white powder (9.10 g, 16.9 mmol, 85% yield). Complete dehydration was confirmed by ^1H NMR and IR spectroscopy. $^{19}F\{^1H\}$ NMR (CD_3CN): δ -79.80 (br, OTf-C**F**$_3$) ppm. IR(ATR): 3347 (s), 1659 (m), 1637 (m), 1377 (w), 1248 (s), 1198 (s), 1188 (s), 1031 (s) cm^{-1}.

S3. Synthesis of $Gd(OTf)_3$

Gd_2O_3 (7.25 g, 20 mmol) was added to a solution of triflic acid (12 g in 10 mL H_20, 144 mmol). The suspension was heated at reflux for 17 h until Gd_2O_3 was mostly consumed. The mixture was filtered and washed with H_2O, and the washings were reduced in volume by vacuum filtration to give a white precipitate. $[Gd(Otf)_3(H_2O)_x]$ was washed with hexane (3 x 5 mL), ground with a pestle and mortar and dehydrated *in vacuo* for 24 h at 200 °C to give $Gd(OTf)_3$ as a white powder (8.57 g, 14.2 mmol, 71% yield). Dehydration was confirmed by ^1H NMR and IR spectroscopy. $^{19}F\{^1H\}$ NMR (CD_3CN): δ -80.57 (OTf-C**F**$_3$) ppm. IR(ATR): 1637 (w), 1288 (m), 1199 (s), 1041 (s), 628 (s).

S4. Synthesis of potassium hexafluoroacetylacetonate [K(hfac)]

To a suspension of KH (0.96 g, 23.9 mmol) in THF (10 mL) at -78 ^oC, hexafluoroacetylacetone (5.00 g, 23.9 mmol) was added dropwise *via* cannula over 2 min. The reaction was allowed to warm to room temperature and stirred for 30 min. The pale yellow solution was filtered *via* filter cannula and THF removed *in vacuo*. The off-white solids were washed with hexane (3 x 5 mL), giving potassium hexafluoroacetyacetonate (4.85 g, 18.4 mmol, 84% yield). ^1H NMR (d_8-THF): δ 5.54 (4H, s, hfac-C**H**) ppm. $^{19}F\{^1H\}$ NMR (d_8-THF): δ -77.81 (hfac-C**F**$_3$) ppm.

Spectroscopic data for Complexes 1-6, NMR and ATR-IR:

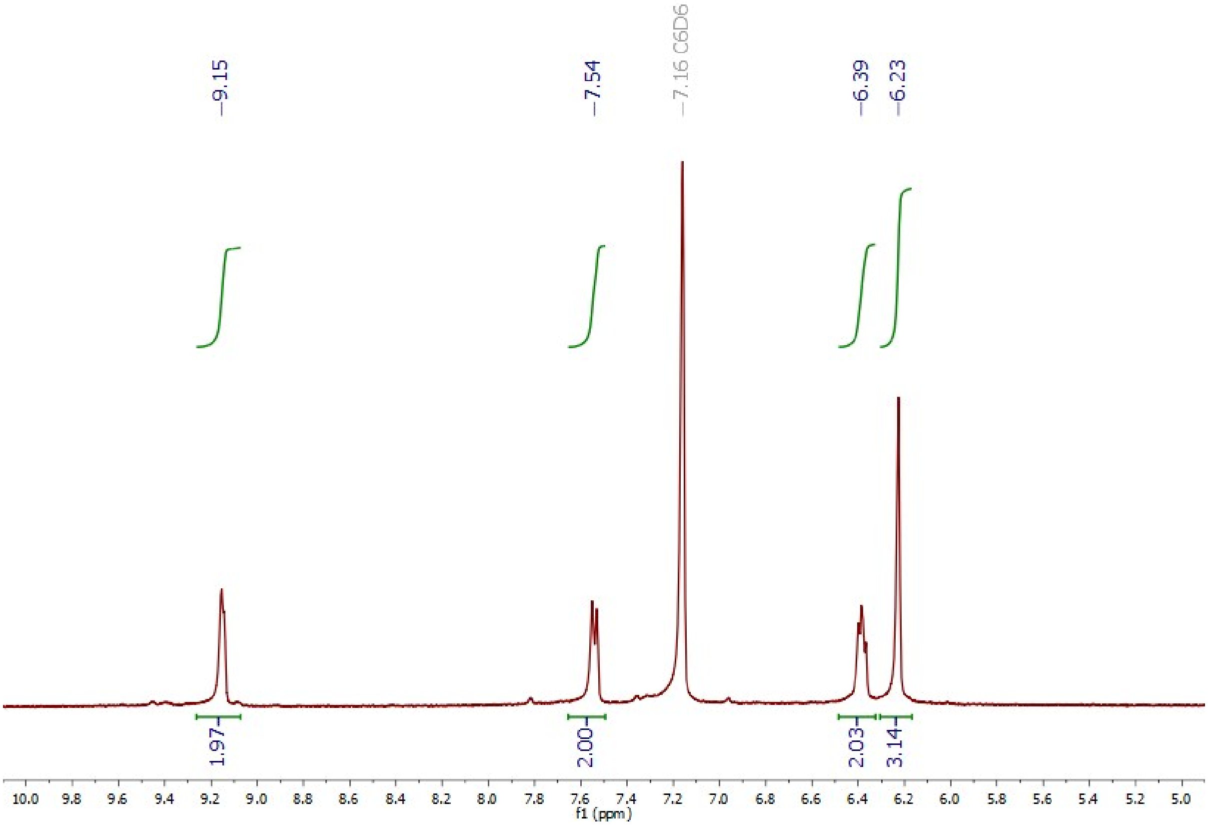

Figure S1. ^{1}H NMR spectrum of **1**, recorded in C_6D_6 at 298 K

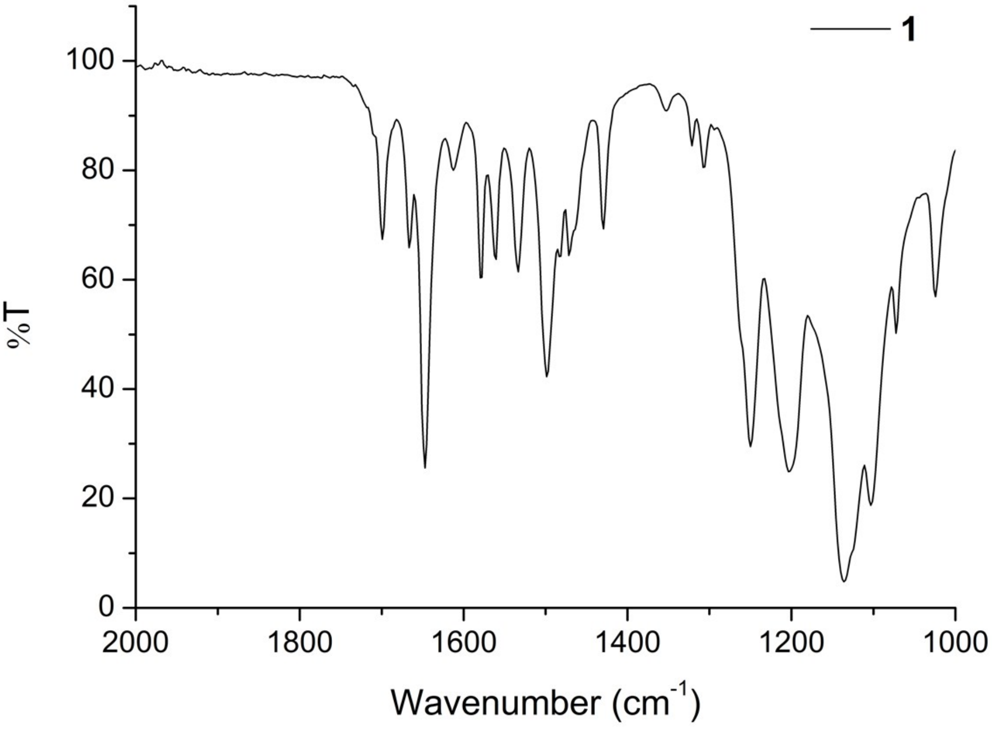

Figure S2. ATR-IR spectrum of **1**, recorded at 298 K

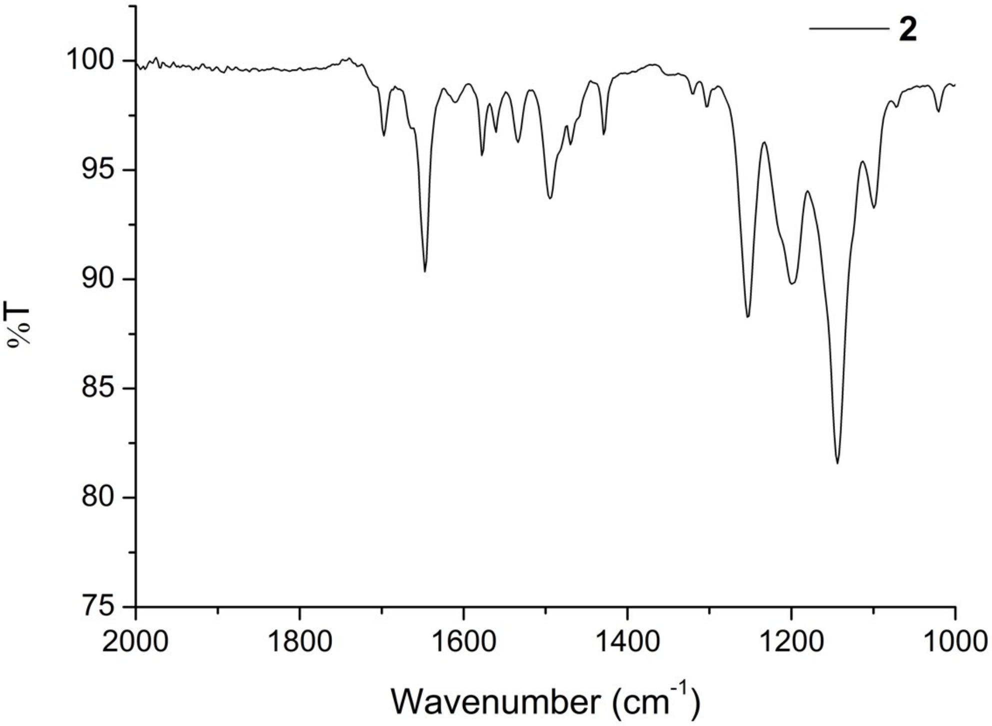

Figure S3. ATR-IR spectrum of **2**, recorded at 298 K

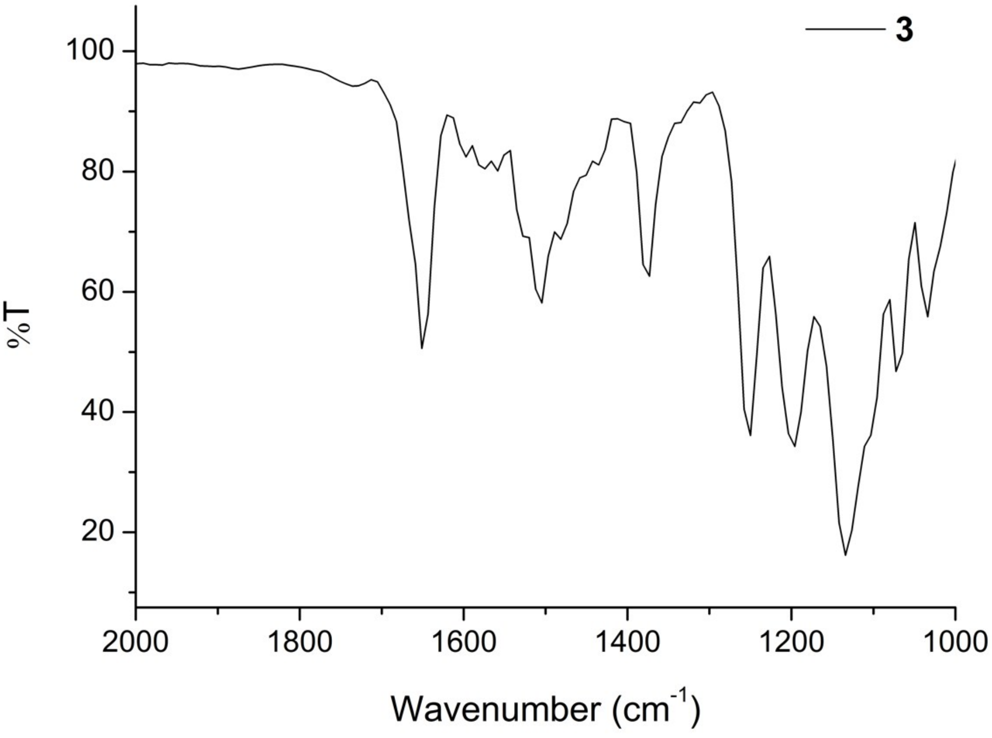

Figure S4. ATR-IR spectrum of **3**, recorded at 298 K

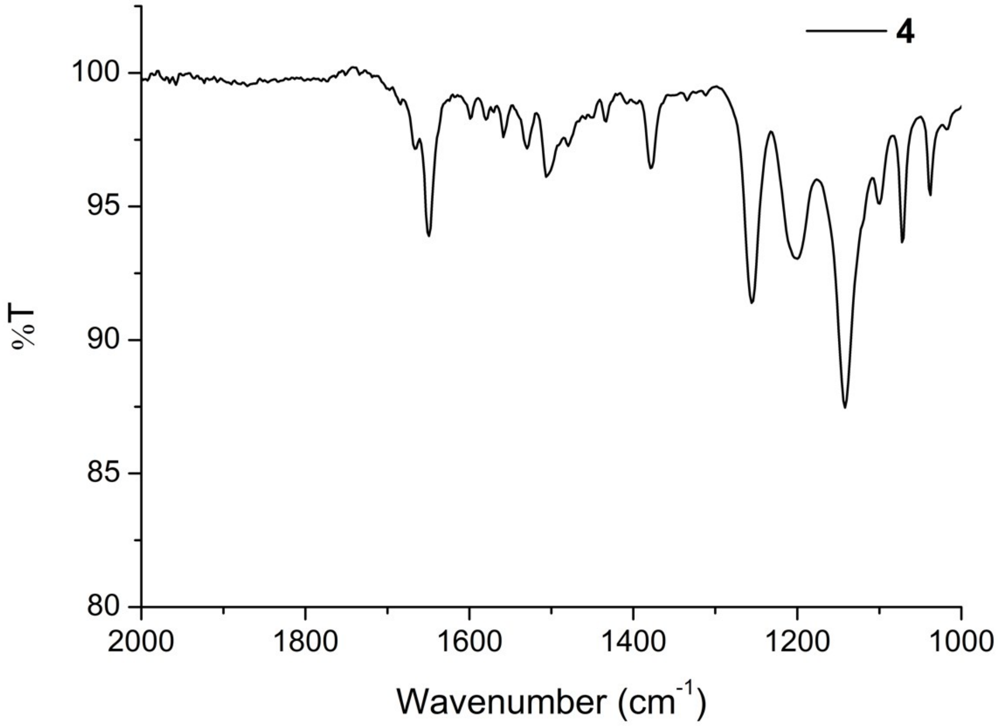

Figure S5. ATR-IR spectrum of **4**, recorded at 298 K

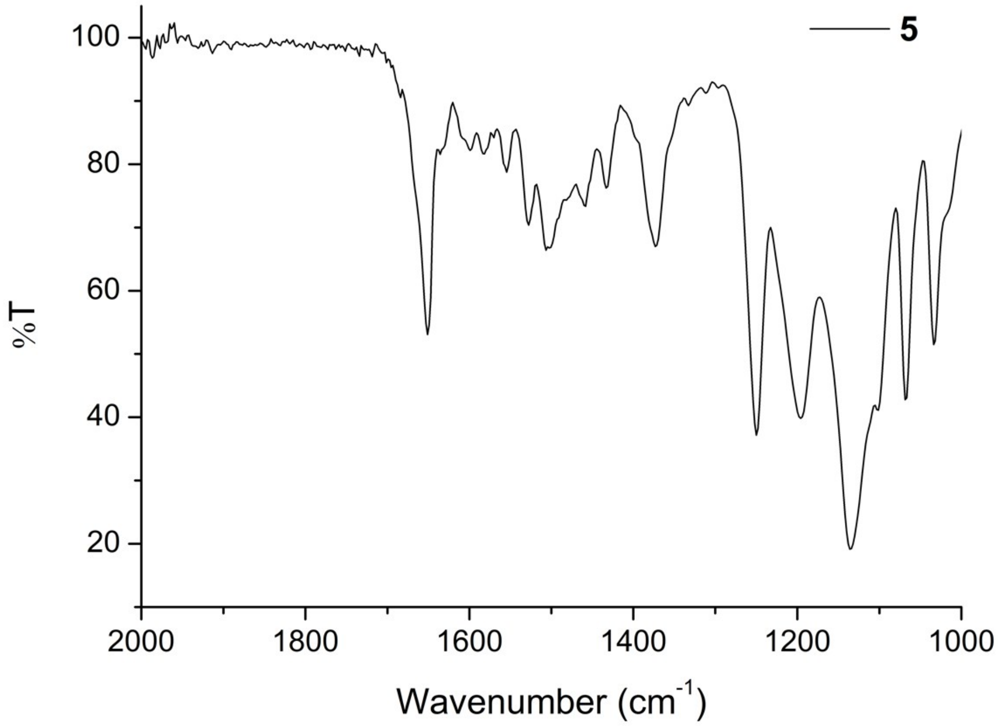

Figure S6. ATR-IR spectra of **5,** recorded at 298 K

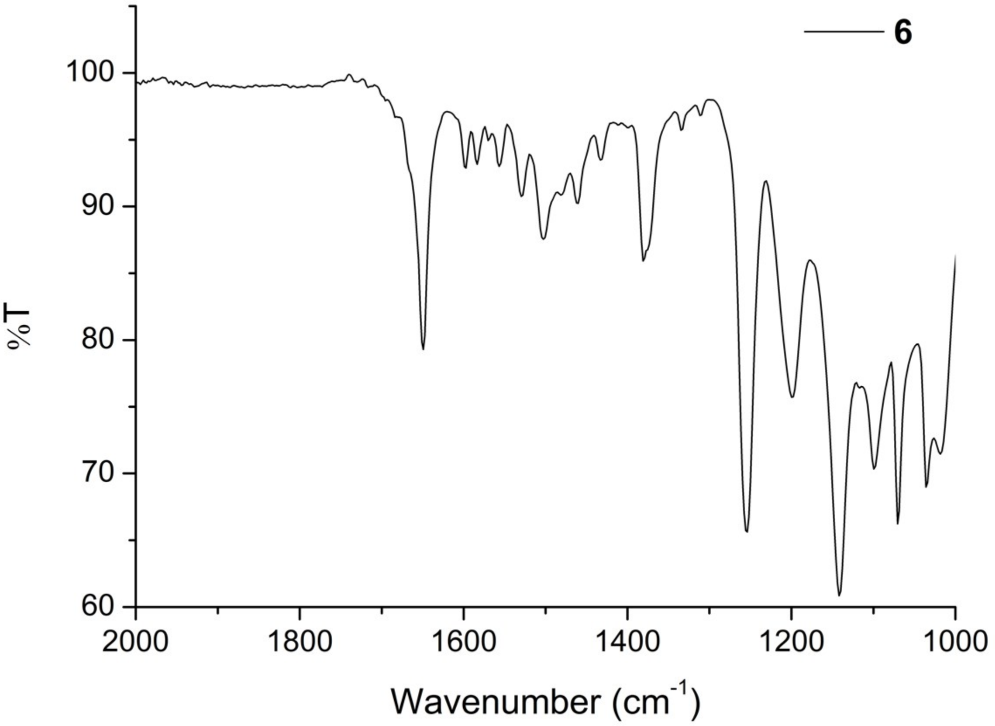

Figure S7. ATR-IR spectrum of **6**, recorded at 298 K

Additional spectroscopic data for Complexes 1-4, UV-vis-NIR:

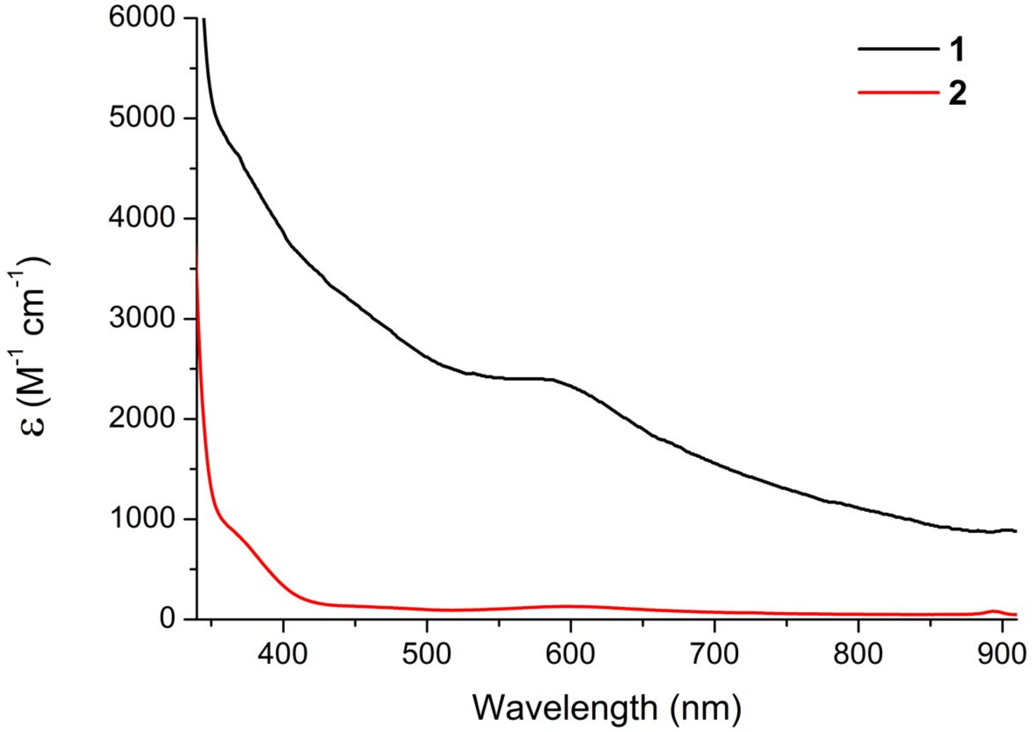

Figure S8. Electronic spectra of 100 µM solutions of **1** and **2**, recorded in MeCN at 298 K

Magnetic Moment Data for Complexes 2, 3, 5 and 6:

Complex	Concentration (M)	Average shift (Hz)	μ_{eff} (μ_B)	μ_{SO} (μ_B)
[Y(hfac)$_3$(*N,N'*-*O,O'*-pd)V(Cp)$_2$] **3**	0.0302	35.1	1.71	1.73
	0.0285	35.0	1.74	
	0.0317	38.2	1.73	
[Y(hfac)$_3$(*N,N'*-*O,O'*-pd)V(Cp^t)$_2$] **5**	0.0218	25.2	1.75	1.73
	0.0308	33.3	1.72	
	0.0285	32.1	1.74	
[Gd(hfac)$_3$(*N,N'*-pd)].Tol **2**	0.0315	1247.0	7.56	7.94
	0.0314	1265.3	7.62	
	0.0204	841.0	7.71	
[Gd(hfac)$_3$(*N,N'*-*O,O'*-pd)V(Cp^t)$_2$] **6**	0.0131	595.7	8.10	8.12
	0.0164	725.4	7.99	
	0.0175	858.9	8.41	

Table S1. Corrected magnetic moment data for **2**, **3**, **5** and **6**. Measurements were taken in d_8-thf at room temperature from crystalline material and magnetic moments calculated according to the Evans Method.[3]

Additional Crystallographic Data:

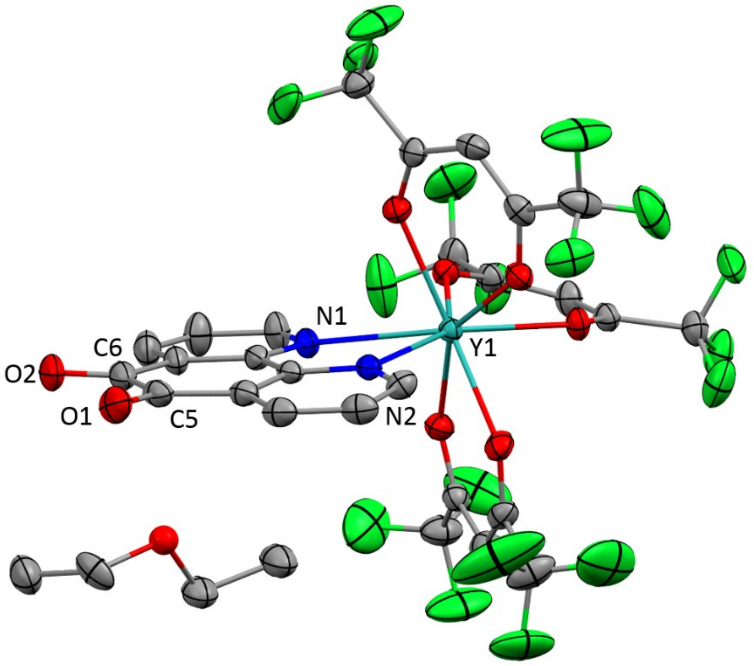

Figure S9. Molecular structure of **1a**. Hydrogen atoms omitted for clarity. Thermal ellipsoids drawn at 50% probability. Selected distances (Å): Y1-N1 2.524(3), Y1-N2 2.520(3), C5-C6 1.535(7), C5-O1 1.224(4), C6-O2 1.220(5).

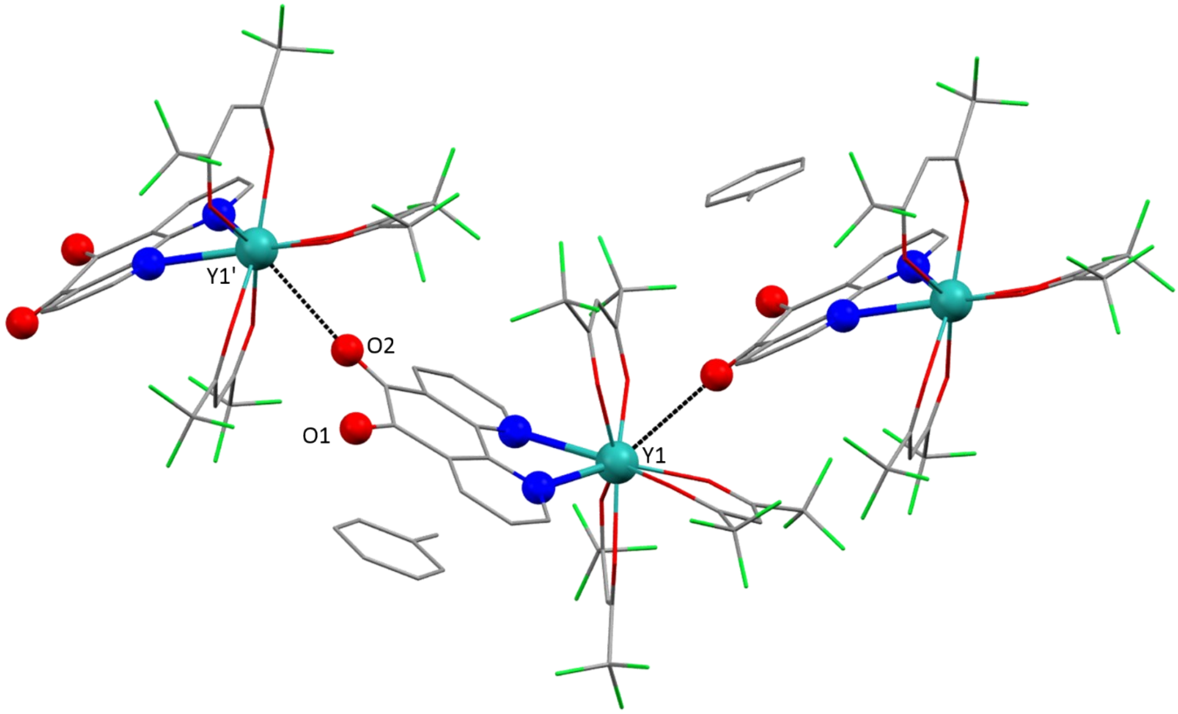

Figure S10. Molecular structure of **1b**, highlighting short contacts between Y1 and O2. Hydrogen atoms omitted for clarity. Structure depicted as wireframe with selected atoms depicted as ball and stick. Selected distance (Å): Y1-O2 3.154.

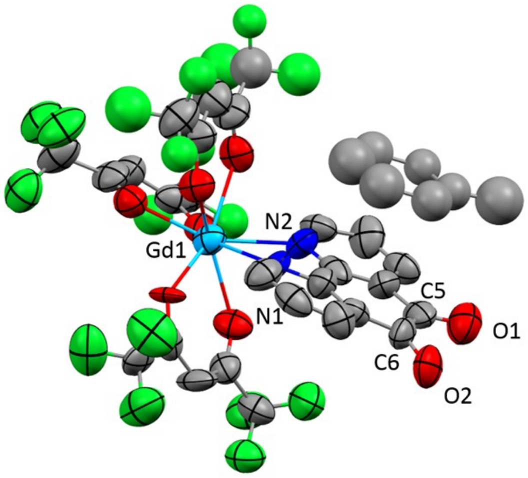

Figure S11. Molecular structure of **2b**. Hydrogen atoms omitted for clarity. Thermal ellipsoids drawn at 50% probability. Selected atoms not refined anisotropically due to disorder. Selected distances (Å): Gd1-N1 2.58(1), Gd1-N2 2.53(2), C5-C6 1.53(3), C5-O1 1.26(3), C6-O2 1.22(3), Gd1-O1 2.84(2).

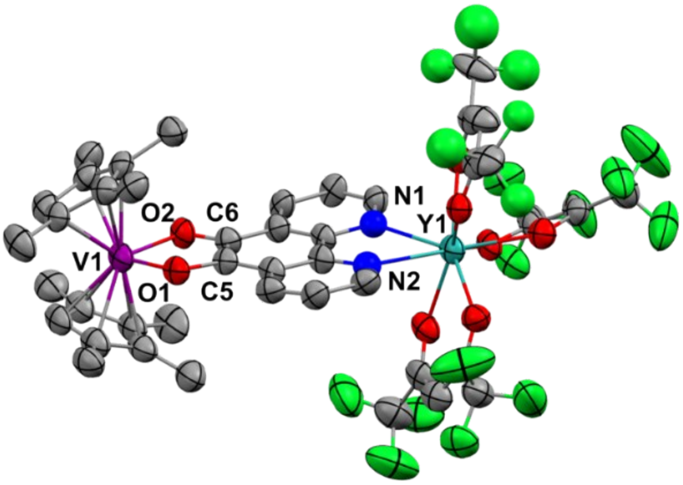

Figure S12. Molecular structure of **5**. Hydrogen atoms and solvent of crystallisation omitted for clarity. Thermal ellipsoids drawn at 50% probability, selected ancillary ligand atoms depicted as ball and stick due to CF_3 disorder. Selected distances (Å): Y1-N1 2.48(1), Y1-N2 2.49(1), C5-C6 1.38(2), C6-O2 1.35(1), C5-O1 1.34(2), V1-O1 1.975(8), V1-O2 1.977(9).

EPR data for 2:

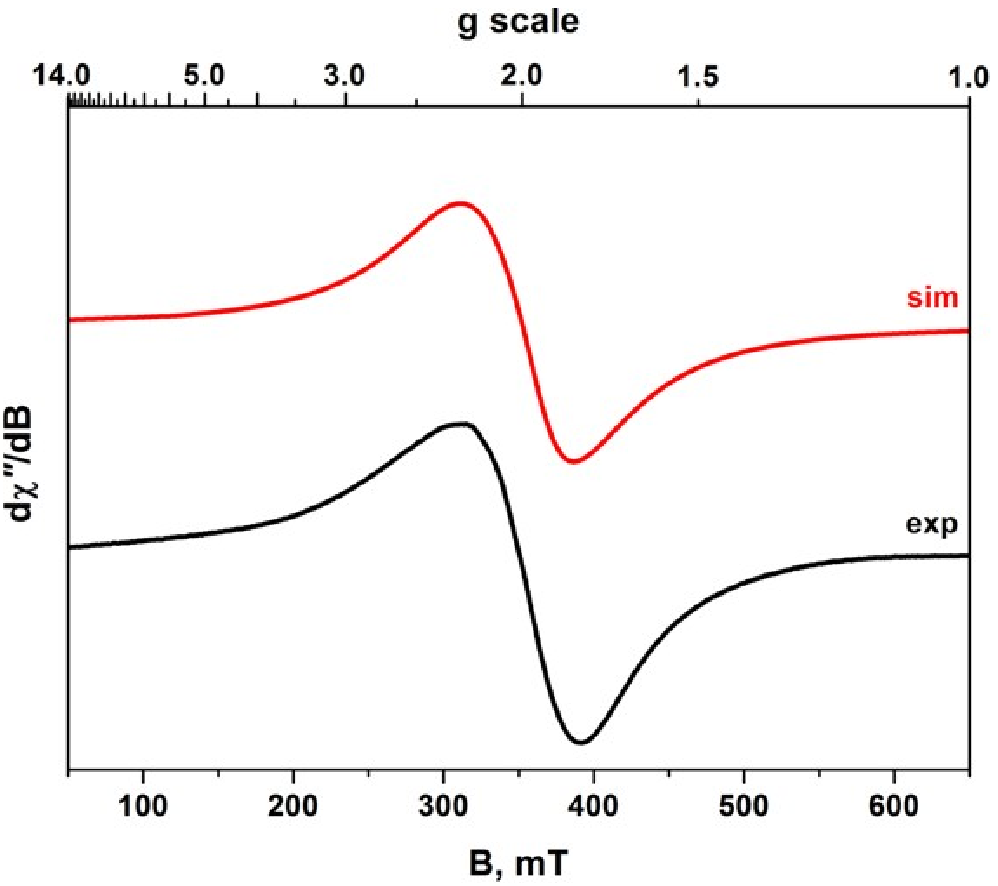

Figure S13. X-band EPR spectrum of **2** recorded in toluene solution at 293 K (experimental conditions: frequency, 9.8623 GHz; power, 0.63 mW; modulation, 0.3 mT). Experimental data are represented by the black line; simulation is depicted by the red trace.

Computational details:

Calculations. The program package ORCA was used for all calculations.[4] The input geometry was generated using ArgusLab, and then optimised via a spin-unrestricted DFT method employing the BP86 functional[5] with acetonitrile as solvent. Split-valence basis sets with one set of polarization functions (def2-SVP) were used for all atoms.[6,7] A scalar relativistic correction was applied using the zeroth-order regular approximation (ZORA) method[8] as implemented by van Wüllen.[9] The RI-J approximation combined with the appropriate Ahlrichs auxiliary basis set was used to speed up the calculations.[10] The conductor like screening model (COSMO) was used for all calculations.[11] The self-consistent field calculations were tightly converged (1×10^{-8} E_h in energy, 1×10^{-7} E_h in the charge density, and 1×10^{-7} in the maximum element of the DIIS[12] error vector). The geometry was converged with the following convergence criteria: change in energy $<10^{-5}$ E_h, average force $<5 \times 10^{-4}$ E_h Bohr^{-1}, and the maximum force 10^{-4} E_h Bohr^{-1}. The geometry search for all complexes was carried out in redundant internal coordinates without imposing geometry constraints.

Electronic property calculations at the optimised geometry were done with the PBE0 functional.[14] The scalar relativistically recontracted ZORA-def2-TZVP(-f) were used all atoms and enhanced integration accuracy was used for the metal atoms (SPECIALGRIDINTACC 10).[7,14] Calculations employed the RIJCOSX algorithm to speed the calculation of Hartree–Fock exchange.[15] TD-DFT calculations were carried out as described by Neese and Olbrich.[16] The first 80 states were calculated where the maximum dimension of the expansion space in the Davidson procedure (MAXDIM) was set to 800. The full width at half maximum (FWHM) was set to 4500 cm^{-1}. Molecular orbitals and spin density maps were visualised via the programme Molekel.[17]

Table S2. Comparison of Experimental and Calculated Bond Distances (Å)

	3		5
	Exptl	Calcd	Exptl
Y–N(1)	2.47(2)	2.550	2.48(1)
Y–N(2)	2.48(2)	2.551	2.49(1)
V–O(5)	1.97(2)	1.960	1.975(8)
V–O(6)	1.97(2)	1.960	1.977(8)
V–C_{Cp}	2.30(2)	2.362	2.33(1)
O(1)–C(5)	1.40(2)	1.335	1.34(2)
O(2)–C(6)	1.24(2)	1.336	1.35(1)
C(5)–C(6)	1.40(2)	1.391	1.38(2)

Table S3 Geometry-Optimised Coordinates for **3**

Y	8.629904	11.245466	3.083574
V	7.648599	2.777387	2.903399
O	10.431624	11.095750	4.547946
O	10.564478	11.035449	1.787439
C	8.222138	7.925015	2.292931
O	6.316582	10.926984	2.957604
C	8.254291	7.887170	3.744533
O	7.721048	11.993535	5.086989
O	7.790458	4.278605	1.674785
C	8.061451	6.706255	1.548506
N	8.351197	9.130671	1.672769
N	8.408891	9.060504	4.417472
O	7.834292	4.214341	4.199189
C	7.935825	5.465802	2.264083
C	8.129337	6.632082	4.434914
C	7.967180	5.429499	3.665164
C	8.453668	9.051570	5.754681
C	8.323463	9.187446	0.337113
C	8.040668	6.792006	0.130948
C	8.175126	6.649562	5.854666
C	11.811305	11.007512	2.006337
C	11.691642	11.064796	4.452921
C	12.681398	10.914261	0.735350
C	12.448673	11.036376	3.262789
C	8.339843	7.861962	6.514572
C	8.170200	8.036305	-0.473825
C	6.573338	12.033419	5.617873
C	5.329480	11.089802	3.729926
C	6.566130	12.561359	7.067906
C	5.356385	11.624436	5.036421
C	12.434599	11.033746	5.805338
C	3.974697	10.627057	3.151139
F	4.024823	9.308431	2.876002
F	3.707666	11.283498	2.009963
F	2.953519	10.835704	4.007990
F	5.328204	12.585224	7.602349
F	7.073185	13.801067	7.119046
F	7.336215	11.759640	7.839033
F	12.116000	12.114047	6.535552
F	13.774843	11.003786	5.654382
F	12.067728	9.935390	6.498239
F	12.419209	11.948853	-0.081562
F	14.001407	10.918974	1.012527
F	12.397559	9.775224	0.072257
O	8.037771	12.145254	1.025055
O	9.236186	13.481518	3.139926

C	9.361999	14.400356	2.280929
C	8.334919	13.207548	0.401812
C	9.976112	15.710310	2.821365
C	8.983223	14.343357	0.921972
C	7.882679	13.224945	-1.072595
F	9.162940	16.241137	3.752306
F	11.167258	15.463221	3.391677
F	10.156523	16.628037	1.847932
F	8.320279	12.109981	-1.699913
F	6.539702	13.239006	-1.143984
F	8.353016	14.291672	-1.746039
C	9.968147	2.776577	2.498146
C	9.799740	2.350155	3.838576
C	9.341225	1.813339	1.641884
C	9.070340	1.124316	3.831050
C	8.829323	0.770467	2.466182
C	5.930481	1.400941	1.981194
C	6.048889	1.073194	3.368891
C	5.511446	2.758567	1.888151
C	5.753664	2.242612	4.124971
C	5.400119	3.280176	3.204301
H	8.582189	10.025500	6.242140
H	8.412360	10.186017	-0.106597
H	7.922438	5.872951	-0.454922
H	8.079775	5.703287	6.399970
H	13.538067	11.009948	3.317384
H	8.381574	7.915256	7.608611
H	8.154742	8.145345	-1.564440
H	4.428854	11.715820	5.602698
H	9.164513	15.203109	0.275780
H	10.421634	3.717447	2.179401
H	10.098395	2.908607	4.727917
H	9.287361	1.864957	0.551212
H	8.779790	0.546993	4.712284
H	8.325660	-0.132961	2.116712
H	6.109777	0.728544	1.138327
H	6.338259	0.102859	3.778061
H	5.378162	3.325484	0.964872
H	5.790329	2.337747	5.212977
H	5.158013	4.312712	3.464921

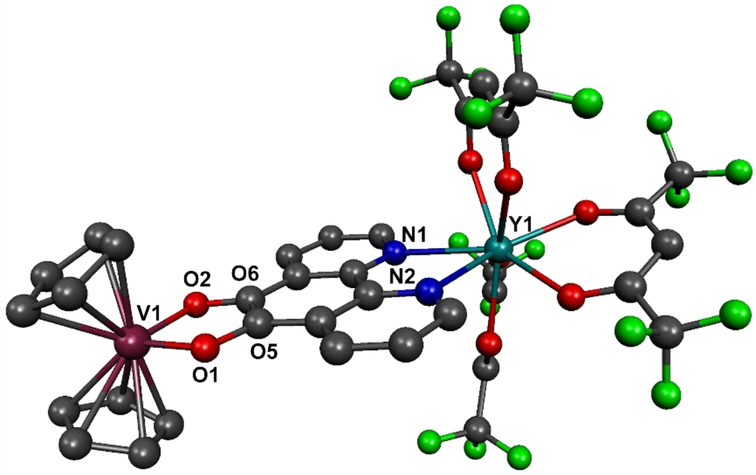

Figure S14. Geometry optimized structure of **3**

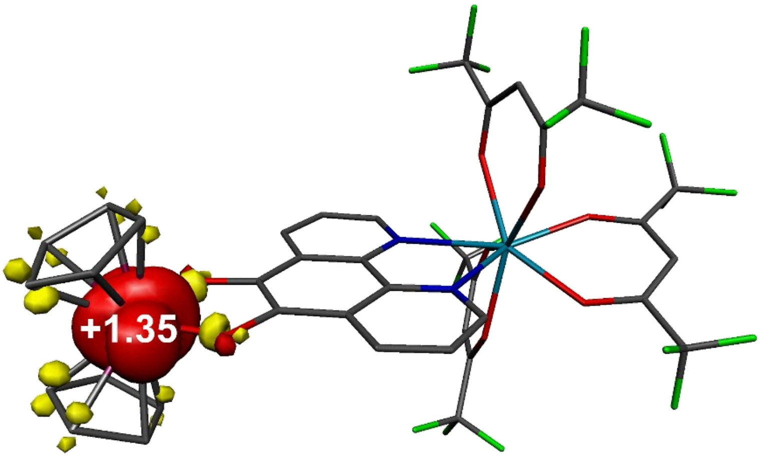

Figure S15. Mulliken spin density plot of **3**

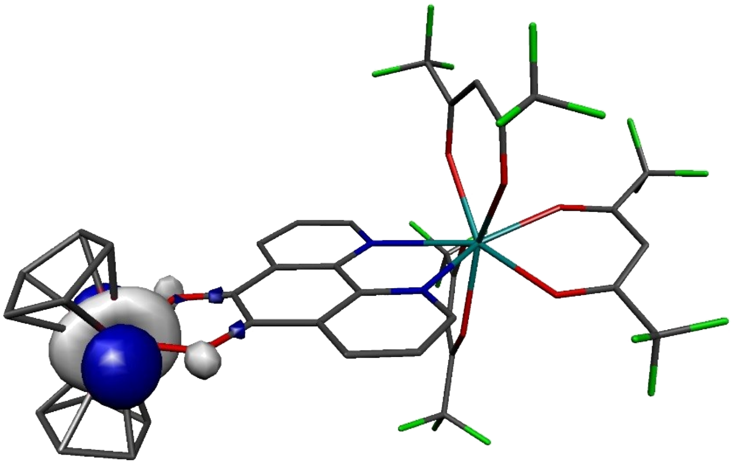

Figure S16. The ground state SOMO for **3**

References

1. Yamada, M., Tanaka, Y., Yoshimoto, Y., Kuroda, S., Shimao, I., *Bull. Chem. Soc. Jpn.* **1992,** *65,* 1006-1011.
2. Fukuzumi, S.; Fujii, Y.; Suenobo, T., *J. Am. Chem. Soc.* **2001,** *123*, 10191.
3. Sur, S. K. *J. Magn. Reson.*, **1989**, *82*, 169.
4. Neese, F. *WIREs Comput. Molec. Sci.*, **2012**, *2*, 73–78.
5. (a) A. D. Becke, *Phys. Rev. A*, **1988**, *38*, 3098–3100. (b) J. P. Perdew, *Phys. Rev. B*, **1986**, *33*, 8822–8824.
6. R. Ahlrichs and K. May, *Phys. Chem. Chem. Phys.*, **2000**, *2*, 943–945.
7. F. Weigend and R. Ahlrichs, *Phys. Chem. Chem. Phys.*, **2005**, *7*, 3297–3305.
8. (a) E. van Lenthe, J. G. Snijders and E. J. Baerends, *J. Chem. Phys.*, **1996**, *105*, 6505–6516. (b) E. van Lenthe, S. Faas and J. G. Snijders, *Chem. Phys. Lett.*, **2000**, *328*, 107–112. (c) E. van Lenthe, A. van der Avoird and P. E. S. Wormer, *J. Chem. Phys.*, **1998**, *108*, 4783–4796.
9. C. van Wüllen, *J. Chem. Phys.*, **1998**, *109*, 392–399.
10. (a) K. Eichkorn, O. Treutler, H. Öhm, M. Häser and R. Ahlrichs, *Chem. Phys. Lett.*, **1995**, *242*, 652–660. (b) K. Eichkorn, F. Weigend, O. Treutler and R. Ahlrichs, *Theor. Chem. Acc.*, **1997**, *97*, 119–124.
11. A. Klamt and G. Schüürmann, *J. Chem. Soc., Perkin Trans. 2,* **1993**, 799–805.
12. (a) P. Pulay, *Chem. Phys. Lett.*, **1980**, *73*, 393–398. (b) P. Pulay, *J. Comput. Chem.*, **1982**, *3*, 556–560.
13. (a) J. P. Perdew, K. Burke and M. Ernzerhof, *Phys. Rev. Lett.*, **1996**, *77*, 3865–3868. (b) C. Adamo and V. Barone, *J. Chem. Phys.*, **1999**, *110*, 6158–6170.
14. D. A. Pantazis, X.-Y. Chen, C. R. Landis, and F. Neese, *J. Chem. Theory Comput.* **2008**, *4*, 908–919.
15. (a) F. Neese, F. Wennmohs and A. Hansen, *J. Chem. Phys.*, **2009**, *130*, 114108. (b) R. Izsák and F. Neese, *J. Chem. Phys.*, **2011**, *135*, 144105.
16. F. Neese and G. Olbrich, *Chem. Phys. Lett.*, **2002**, *362*, 170–178.
17. *Molekel*, Advanced Interactive 3D-Graphics for Molecular Sciences, Swiss National Supercomputing Centre. https://ugovaretto.github.io/molekel/